Macromolecules

pubs.acs.org/Macromolecules Article

High-Resolution Comonomer Sequencing of Blocky Brominated Syndiotactic Polystyrene Copolymers Using ^{13}C NMR Spectroscopy and Computer Simulations

Kristen F. Noble, Diego Troya, Samantha J. Talley, Jan Ilavsky, and Robert B. Moore*

Cite This: *Macromolecules* 2020, 53, 9539−9552 Read Online

ACCESS | Metrics & More | Article Recommendations | Supporting Information

ABSTRACT: This work demonstrates the first high-resolution comonomer sequencing of Blocky brominated syndiotactic polystyrene (sPS-*co*-sPS-Br) copolymers based on pentad assignments of the quaternary carbon region of the nuclear magnetic resonance spectrum. Copolymers containing *p*-bromostyrene (Br-Sty) units were prepared in matched sets using postpolymerization bromination methods carried out in the heterogeneous gel state (Blocky) and homogeneous solution state (Random). Quantitative information from the quaternary carbon spectra, heteronuclear multiple bond correlation spectroscopy, electronic structure calculations, and simulated statistically random copolymers was correlated to confirm the carbon resonance assignments for all 20 possible pentad comonomer sequences. Using the experimental pentad sequence prevalences, a computer code was developed to simulate chains with microstructures typical of each sample as a means to visually represent the copolymer blockiness with quantitative precision. Based on the microstructure and distribution of run lengths in these chains, the simulations revealed that the Blocky copolymers contain a high degree of blockiness. By comparing the run lengths in the simulated chains to the average number of styrene units in a crystalline segment of sPS (found by small-angle X-ray scattering), copolymer crystallizability was predicted. For the simulated Blocky B-21% (21 mol % Br-Sty) chain, the probability of randomly selecting a styrene unit in a crystallizable block was 25.8%, while that in the simulated Random R-18% was zero, in excellent agreement with the experimental crystallization behavior measured by differential scanning calorimetry. These predictions confirmed that the simulated chains accurately represent the ensemble of chains in their respective copolymer samples. Furthermore, each simulated Blocky chain contained one or more long sPS blocks that paralleled the measured 38−40 styrene units spanning a crystalline segment within the sPS/CCl_4 gel. This finding affirmed that the long sPS segments originated from the precise lamellar structure within the heterogeneous gel morphology (i.e., block length is correlated with lamellar thickness). Overall, the ability to tailor the copolymer microstructure through control of the semicrystalline gel morphology opens the door to synthesizing ordered copolymers by postpolymerization functionalization processes with unprecedented levels of compositional control.

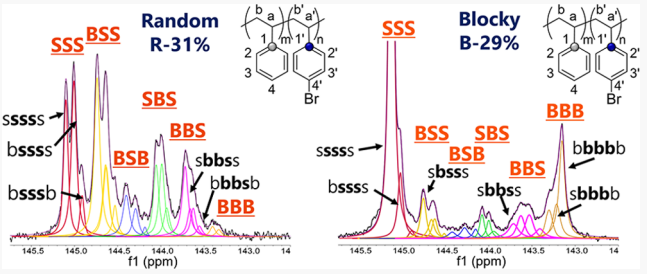

INTRODUCTION

The physical properties of copolymers depend on the microstructure of the polymer chains, i.e., the tacticity of the repeating units and the sequence distribution of the comonomers.[1−6] In pure syndiotactic polystyrene (sPS), for example, the styrene units are arranged in a regular stereochemical configuration, such that the phenyl rings alternate in racemic diads with respect to the carbon backbone. The tactic purity of sPS is confirmed by sharp signals in the ^{13}C nuclear magnetic resonance (NMR) spectrum. This stereoregularity allows the chain segments to adopt ordered conformations that are capable of forming crystalline domains within a semicrystalline network. To tailor the physical properties of this inherently nonpolar polymer, a number of functional copolymers of sPS have been synthesized by either copolymerization or postpolymerization modification.[7−12] Consequently, however, these functional comonomers can act as physical defects along the polymer chain, which severely limits the copolymer crystallizability.[7,13,14]

Recently, we introduced a new postpolymerization functionalization method carried out in the heterogeneous gel state that is capable of preparing copolymers with a blocky microstructure that preserves crystallizability at a relatively high functional group content (e.g., 29 mol % functionalized units).[13] Gels of crystallizable polymers (e.g., sPS) are composed of tightly packed chain segments in lamellar crystallites that act as physical cross-links bound together by

Received: July 15, 2020
Revised: October 14, 2020
Published: October 27, 2020

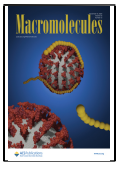

https://dx.doi.org/10.1021/acs.macromol.0c01630
Macromolecules 2020, 53, 9539−9552

a percolating network of solvent-swollen amorphous chains.[15−20] In our gel-state functionalization process, the functionalizing reagent is believed to be excluded from the crystalline component of the gel network and thus accessible only to monomers in the amorphous component between crystallites.[13,21,22] This preferential functionalization thus preserves long, crystallizable runs of consecutive monomer units that were inaccessible to the functionalizing reagents within the tightly packed crystalline lamella of the heterogeneous reaction medium. Copolymers formed by this new postpolymerization process exhibit significantly greater crystallizability and crystallize faster than their random copolymer analogues prepared by a conventional, homogeneous, solution-state functionalization method.[13,22] This enhanced crystallization behavior is attributed to a significant degree of nonrandomness in the distribution of comonomers along the copolymer chain, which herein will be described as a copolymer with a "blocky" microstructure.

To develop a deeper understanding of the relationship between the homopolymer/solvent gel morphology and the resulting copolymer microstructure of the gel-state functionalized copolymers, a high-resolution, quantitative measure of the copolymer sequence, as offered by ^{13}C NMR spectroscopy, is required. For pure polystyrene, the NMR signal of the phenyl ring quaternary (C(1)) carbon in atactic polystyrene (aPS) and its phenyl ring-substituted derivatives exhibits high sensitivity to monomer configuration (i.e., tacticity),[23−30] composition,[31,32] and comonomer sequence distribution.[6,14,33,34] Nevertheless, due to complexities in the C(1) resonances that arise from stereoirregularity and the chemical similarity of para-substituted styrene monomers, attempts by others to evaluate the comonomer sequence distribution of atactic polystyrene (aPS)-based copolymers by NMR have been generally unsuccessful.[2,35−41] Fortunately, for stereoregular syndiotactic polystyrene with high tactic purity, the spectral complexity of the brominated syndiotactic polystyrene (sPS-*co*-sPS-Br) copolymers used in this study is greatly reduced. Thus, the quaternary carbon resonances for styrene (C(1)) and brominated styrene (Br-Sty, C(1′)) monomers in this stereoregular model system are now recognized to be sensitive to neighboring monomers, which permits precise copolymer sequencing.[6,14,32]

Assignment of the C(1) resonances to stereosequences, or, for some syndiotactic polystyrene copolymers, diad or triad comonomer sequences, has been achieved by comparing the relative peak areas of the C(1) resonances to either Bernoullian[26−30] (i.e., statistically random) or first- or second-order Markovian (i.e., random sequence distribution based on probability parameter) models.[6,14,42] For example, Cui et al.[14] were recently able to assign the C(1) resonances in a syndiotactic styrene-*co*-4-methylthiostyrene copolymer to triad combinations of monomers based on the conformity of the relative peak areas to first-order Markov statistics. These statistical models are particularly relevant for random copolymers prepared by direct polymerization methods, where the catalyst and monomer reactivity ratio often control the stereoregularity and composition of the growing polymer chain. Systematic changes to the monomer feed ratio or reaction time affect monomer conversion. Thus, the changes in relative peak areas observed in the ^{13}C NMR spectrum can be compared to statistical probabilities to make peak assignments.[6,14,42] For some copolymers, two-dimensional (2D) heteronuclear NMR spectroscopy techniques have proven useful for identifying peaks that arise from specific monomers.[33,39,40] Model compounds of polystyrene and its derivatives (e.g., oligomers of the parent polymer) have also been used to assign stereosequences of the C(1) resonance.[23,31]

In addition to the NMR methods used for investigating copolymer microstructure from direct polymerization, the simulation of polymer chains has proven to be complementary in the investigation of copolymer microstructure from postpolymerization functionalization methods.[5,24,43,44] For example, Harwood et al.[24,45,46] simulated polymer epimerization using a Monte Carlo method and counted the number frequency of triad combinations in the theoretical epimerized chains to assign triad sequences in partially epimerized isotactic polystyrene (iPS) samples. Similarly, using Bernoullian and hemi-isotactic statistical methods to simulate homopolymer chains with a broad range of isotactic content, Miller[47] was able to predict the elastomeric properties of polypropylene (PP) samples based on the block length distributions of the simulated PP chains and the experimental pentad sequence distributions of PP copolymers.

Using the distribution of comonomer sequences obtained from the relative area of the peaks in the ^{13}C NMR spectrum, the copolymer block character (i.e., blockiness) and average block length of consecutive like monomers may be determined based on Bernoullian statistics.[48−50] These calculated values are a useful addition to comonomer sequencing in that they provide deeper insight into the copolymer microstructure, which may help to explain observed differences in copolymer crystallization behavior and morphological development for samples with similar comonomer content.

In this work, ^{13}C NMR spectroscopy is used to investigate the copolymer microstructure and comonomer sequence distribution of brominated sPS copolymers prepared by a postpolymerization functionalization method carried out in the heterogeneous gel state. This work reports the first high-resolution comonomer sequencing of sPS-*co*-sPS-Br copolymers based on pentad assignments of the quaternary carbon region of the quantitative ^{13}C NMR spectrum. Using the experimental pentad sequence prevalences, a computer code was developed to simulate chains with microstructures typical of each sample as a means of visually representing the copolymer blockiness with quantitative precision. The purpose of this research was to develop a comonomer sequencing method for brominated sPS copolymers to obtain a deeper understanding of the relationship between the sPS/solvent gel morphology and the resulting copolymer microstructure and degree of blockiness originating from the gel-state, postpolymerization functionalization process.

MATERIALS AND METHODS

Sample Preparation. To develop the comonomer sequencing method, two series of copolymers were prepared in matched sets containing 6−30 mol % *p*-bromostyrene units using a postpolymerization functionalization method carried out in the homogeneous solution state (Random) and the heterogeneous gel state (Blocky). The preparation of the Random and Blocky sPS-*co*-sPS-Br copolymers is described in a previous publication.[13] Briefly, the Random copolymers (R-*x*%) were prepared by introducing a stock solution of bromine (Br_2) in 1,1,2,2-tetrachloroethane (TCE) to a solution of sPS homopolymer (Questra 102; weight average molecular weight, M_w = 300 000 g mol^{-1}) in TCE containing a Lewis acid catalyst ($FeCl_3$, 5 mol % based on the amount of Br_2). The reaction was carried out in the dark under argon, and the molar ratio of Br_2 to

https://dx.doi.org/10.1021/acs.macromol.0c01630
Macromolecules 2020, 53, 9539−9552

styrene units was varied to control the degree of bromination. The Random copolymers were found to contain Br-Sty compositions of approximately x = 6, 16, 18, and 31 mol %, as determined by ^{1}H NMR spectroscopy. The Blocky copolymers (B-x%) were prepared by introducing a stock solution of Br_2 in 1,2-dichloromethane (DCM) to small pieces of a 10% w/v sPS/carbon tetrachloride (CCl_4) gel suspended in DCM, also containing a Lewis acid catalyst ($FeCl_3$, 68 mg, 0.42 mmol). The reaction was carried out in the dark under argon, and the reaction time was varied to control the degree of bromination. The Blocky copolymers were found by ^{1}H NMR to contain Br-Sty compositions of approximately x = 6, 15, 21, and 29 mol %.

A 10% w/v sPS/CCl_4 gel was prepared for ultra-small-angle and small-angle X-ray scattering (USAXS and SAXS) experiments by dissolving sPS pellets in CCl_4 at 120−140 °C in a pressure vessel, capturing a fraction of the 10% w/v sPS/CCl_4 solution in a thin-walled, 3 mm outer diameter glass tube and removing from heat to promote gel formation. A 10% w/v sPS/CCl_4 gel was prepared for wide-angle X-ray diffraction (WAXD) experiments by dissolving sPS pellets in CCl_4 at 120−140 °C in a pressure vessel, followed by removing from heat to promote gel formation. The gel was stored at room temperature for ca. 24 h to mimic the conditions prior to gel-state bromination. Then, the gel was broken into pieces with a spatula and immediately dried under vacuum at 70 °C for ca. 24 h.

NMR Spectroscopy. Microstructure analysis and comonomer sequencing of the sPS-*co*-sPS-Br copolymers were carried out using NMR spectroscopy. ^{1}H−^{13}C band-selective gradient heteronuclear multiple bond correlation (bsgHMBC) experiments were recorded at room temperature in 1,1,2,2-tetrachloroethane-d_2 (TCE-d_2) on an Agilent U4-DD2 400 MHz spectrometer. Spin−lattice relaxation time, T_1, experiments for ^{13}C were performed at room temperature in TCE-d_2 on a Bruker Avance II 500 MHz NMR spectrometer equipped with an LN_2 prodigy cryogenic broad-band observe (BBO) probe using inversion recovery with a power-gated decoupling pulse sequence (t1irpg). This pulse program produced a serial file (parameter mode = 2D); therefore, the T_1 experiment was carried out in a 2D mode with a size of fid (32768, 9), eight scans per increment, a 40 s relaxation delay, and nine variable delays (0.1, 0.2, 0.4, 0.8, 1.6, 3.2, 6.4, 12.8, 25.6 s) from the variable delay list. The acquired data was processed using Topspin 3.2 software, and T_1 was calculated by an area-fitting method. The calculated T_1 values for the quaternary carbon of sPS homopolymer (C(1)) and a Random R-93% copolymer (C(1′)) were 0.68 and 0.71 s, respectively. Quantitative ^{13}C NMR experiments were recorded at room temperature in TCE-d_2 on a Bruker Avance II 500 MHz spectrometer equipped with an LN_2 prodigy cryogenic BBO probe using a C13IG pulse program, proton decoupling (NOE−), 6 s relaxation delay, 7680 scans per increment, an O1P of 95, and a sweep width of 150 ppm. The line fitting function in Mestrelab Research's MestReNova x64 software was used to deconvolute and integrate the multiple peaks in the quaternary carbon region of the ^{13}C NMR spectrum. The deconvolution method is discussed in more detail in the Results and Discussion section.

Theoretical Quaternary Carbon Chemical Shifts. Theoretical chemical shifts of the quaternary carbon nuclei in the six unique triad sequences were computed using electronic structure calculations. The calculation model consisted of three consecutive monomers terminated by two ethyl capping units. Geometry optimizations and harmonic frequencies were obtained using the B3LYP density functional and the def2-SVP basis set as implemented in Gaussian 09.[51] NMR shielding tensors were computed using the Gauche Invariant Atomic Orbital formalism also in Gaussian. The reported chemical shifts for the quaternary carbon nuclei of the central monomer in the triads were obtained via reference to the isotropic shielding of an internal tetramethylsilane standard calculated at the same level of theory.

Thermal Properties. Copolymer crystallinity was probed by differential scanning calorimetry (DSC, TA Instruments DSC Q2000) under continuous nitrogen flow. The samples were first annealed at 300 °C (325 °C for Blocky B-29%) for 3 min to erase thermal history, then cooled to 0 °C at −10 °C min^{-1}, followed by a 10 °C min^{-1} heat to observe the melting endotherm. TA Instruments Universal Analysis software was used to determine the area under the melting endotherm (ΔH_f).

X-ray Scattering and Diffraction. X-ray scattering techniques were used to characterize the morphology of a 10% w/v sPS/CCl_4 gel. USAXS and SAXS measurements were collected at beamline 9-ID-C at the Advanced Photon Source (APS) at Argonne National Laboratory (Lemont, Illinois).[52] The USAXS instrument was configured in standard mode with an X-ray energy of 21 keV (λ = 0.5895 Å), an X-ray photon flux of ca. 10^{13} mm^{-2} s^{-1}, and a combined scattering vector, q, range of 0.0001−1.3 Å^{-1} ($q = 4\pi/\lambda \sin(\theta)$, where λ is the wavelength and θ is one-half of the scattering angle). The desmeared USAXS and SAXS profiles were acquired sequentially. Data were reduced using the Indra and Nika programs for Igor Pro[53] and normalized in terms of absolute intensity by the USAXS instrument. The Irena program for Igor Pro was used to merge the same-specimen USAXS and SAXS as well as to analyze the data.[54] Additional SAXS experiments were performed on melt-crystallized samples of the sPS homopolymer and the Random and Blocky copolymers using a Rigaku S-Max 3000 3 pinhole SAXS system equipped with a rotating anode that emits X-rays with a wavelength of 0.154 nm (Cu Kα). The sample-to-detector distance was 1605 mm, and the q range was calibrated using a silver behenate standard. Two-dimensional SAXS patterns were obtained using a fully integrated 2D multiwire, proportional counting, and a gas-filled detector with an exposure time of 2 h. The SAXS data were analyzed using the SAXSGUI software package to obtain radially integrated SAXS intensity versus q profiles. The center-to-center intercrystalline domain spacing, i.e., long period (L_p), and average crystal thickness were calculated from the crystalline scattering feature of Lorentz-corrected SAXS profiles using the one-dimensional (1D) correlation function and a linear two-phase model. WAXD experiments were performed using a Rigaku MiniFlex II X-ray diffractometer emitting X-rays with a wavelength of 0.154 nm (Cu Kα). The samples were scanned from 5 to 40° 2θ at a scan rate of 0.250° 2θ min^{-1} and a sampling window of 0.050° 2θ at a potential of 30 kV and a current of 15 mA. The WAXD data were analyzed using the PDXL 2 software package to obtain WAXD intensity versus 2θ profiles. The degree of crystallinity, $\%X_c$ by volume, was calculated from the WAXD profile by integration of the crystalline and amorphous contributions, according to the below equation

$$\%X_c = \frac{I_c}{I_c + I_a} \times 100 \quad (1)$$

where I_c and I_a are the integrated intensities of the crystalline and amorphous contributions, respectively. For each WAXD profile, the crystalline reflections were individually fit using Gaussian functions. The amorphous halo profile was obtained from a melt-quenched amorphous sPS sample.

Comonomer Sequence Counting in Simulated Random Copolymer Chains. Simulated random copolymer chains (r-x%, x = mol % Br) were generated using a code created in-house with MATLAB R2017a programming software.[13] For each desired Br-content, the code simulated 1000 homopolymer chains of 1442 monomer units (based on our sPS sample, M_w = 300 K; $Đ$ = 2.0) and then selected monomers along each chain at random up to the desired degree of bromination. Along each chain, the number of each triad sequence (e.g., SSS, BBB, etc.) and pentad sequence (e.g., SSSSS, BBBBB, etc.) was counted. The prevalence of each of the six unique triad sequences and 20 unique pentad sequences was calculated by dividing the summed occurrences of a particular sequence by the total number of triad or pentad sequences, respectively, in the chain, which is discussed in more detail in the Results and Discussion section. Herein, data from the simulated random chains will be referred to by the lowercase random (r-x%) designation, while data from the experimental samples will be referred to by the uppercase Random (R) and Blocky (B) designations.

Simulated Copolymer Chains Based on the Experimental Pentad Sequence Distributions. Simulated chains that represent a typical copolymer chain within each of the Random and Blocky

https://dx.doi.org/10.1021/acs.macromol.0c01630
Macromolecules 2020, 53, 9539−9552

copolymer samples were created using a Fortran code created in-house (see the Supporting Information). Chains were simulated from a short sequence of unfunctionalized styrene units by subsequent additions of short sequences of unfunctionalized and functionalized styrene units to the chain end. The rationalization for the specific short sequence that was added during each addition step was based on the difference between the average pentad sequence distribution of the simulated intermediate chain and the pentad sequence distribution from the NMR data and is discussed in more detail in the Results and Discussion section.

RESULTS AND DISCUSSION

^{13}C NMR Spectroscopy and Comonomer Sequence Distribution. Quantitative ^{13}C NMR spectroscopy was used to investigate the microstructure and comonomer sequence distribution of the solution-state (Random, R-x%) and gel-state (Blocky, B-x%) sPS-*co*-sPS-Br copolymers. For comparison, the Random and Blocky copolymers were prepared in matched sets of approximately x = 6, 15, 20, and 30 mol % brominated styrene (Br-Sty) units, determined from the ^{1}H NMR spectra.[13] Figure 1 compares the high-resolution,

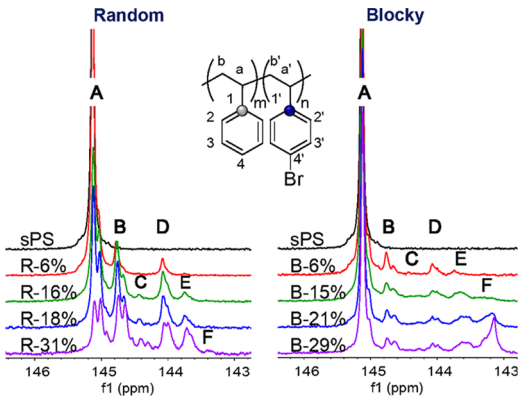

Figure 1. Quaternary carbon region of the ^{13}C NMR spectra for the Random (left) and Blocky (right) copolymers with increasing degree of bromination from top to bottom. The spectra were recorded at room temperature and are referenced to TCE-d_2 and normalized over 127.0−132.5 ppm for comparison.

quaternary carbon (C(1) and C(1′)) NMR spectra of the sPS homopolymer and the Random and Blocky copolymers. The sPS homopolymer exhibits a single peak at 145.15 ppm that corresponds to the C(1) resonance of the unfunctionalized styrene units. Upon para-substitution of the styrene phenyl rings with bromine, new resonances appear upfield in the ^{13}C NMR spectrum. For the Random copolymers, the new peaks increase in intensity with increasing Br-content. The multiple peaks in the sPS-*co*-sPS-Br copolymers originate from through-bond communication between neighboring styrene and Br-Sty monomers, which provide a unique fingerprint of the copolymer microstructure attributed to the specific comonomer sequence distribution.[14,32] For the Blocky copolymers, the quaternary carbon peak distributions and intensities differ discernibly from their Random analogues at all degrees of bromination, which is emphasized by the new resonance in Blocky B-21% and B-29% at 143.1−143.3 ppm. These differences in peak distribution and intensity unambiguously show that copolymers prepared by gel-state bromination have a different comonomer sequence distribution compared to their solution-state analogues.

The peaks in the quaternary carbon region appear to be clustered into six groups, which are labeled A−F in Figure 1 and are clearly observed in the spectrum of Random R-31%. The observed number of groups is in excellent agreement with the six unique triad combinations (eight total combinations) that are possible in a copolymer that contains two different monomers (i.e., SSS, [SSB/BSS], BSB, SBS, [BBS/SBB], and BBB, where S = styrene and B = Br-Sty). Thus, each group is attributed to the quaternary carbon nucleus of a styrene, **S**, or Br-Sty, **B**, unit that exists in the center of a unique sequence of three monomers, i.e., a triad, along the copolymer chain.

To facilitate the assignment of the quaternary carbon resonances as originating from either a central styrene or Br-Sty unit, specific heteronuclear ^{1}H−^{13}C correlations were probed by bsgHMBC spectroscopy. The quaternary carbon and aromatic H(3)/H(4)/H(3′) proton regions of the bsgHMBC spectra for Random R-31% and Blocky B-29% are presented in Figure 2. For both R-31% and B-29%, the

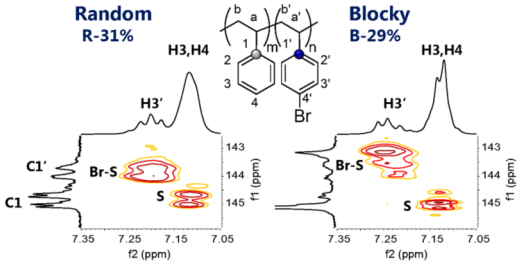

Figure 2. Quaternary carbon region of the bsgHMBC spectra for the Random R-31% (left) and Blocky B-29% (right) copolymers recorded in TCE-d_2 at 25 °C.

quaternary carbon resonances in the 144−145 ppm range are correlated to the H(3) and/or H(4) protons, indicating that these resonances originate from a central unfunctionalized styrene unit, C(1), in a triad. The carbon resonances at lower frequency, in the 143−144 ppm range, are correlated to the H(3′) proton and thus originate from a central Br-Sty unit, C(1′), in a triad. Therefore, groups A−C were assigned to triads containing a central unfunctionalized styrene unit and groups D−F were assigned to triads containing a central Br-Sty unit.

To further assign groups A−F to specific triad sequences of monomers, electronic structure calculations were used to compute theoretical chemical shifts for the quaternary carbon nuclei of the central unit in each of the six unique triad sequences. Figure 3 shows the optimized structure of the six unique triad sequences terminated with ethyl capping units and the computed chemical shifts of each model structure. The density functional theory (DFT)-calculated chemical shift of the quaternary carbon nucleus of the central styrene or Br-Sty unit in each triad sequence decreases in the following order: SSS > [SSB/BSS] > BSB > SBS > [BBS/SBB] > BBB. Thus, the quaternary carbon nucleus of a Br-Sty unit is predicted to resonate at a lower frequency than a styrene unit, consistent with the results from the bsgHMBC experiments (see Figure 2). In addition, the resonance frequency of a styrene or Br-Sty unit decreases with an increasing number of Br-Sty neighbors. This result strongly suggests that bromination of the C(4) carbon of the phenyl ring shields the quaternary carbon nucleus of styrene and neighboring styrene units from the applied external magnetic field. Based on the results of the

https://dx.doi.org/10.1021/acs.macromol.0c01630
Macromolecules 2020, 53, 9539−9552

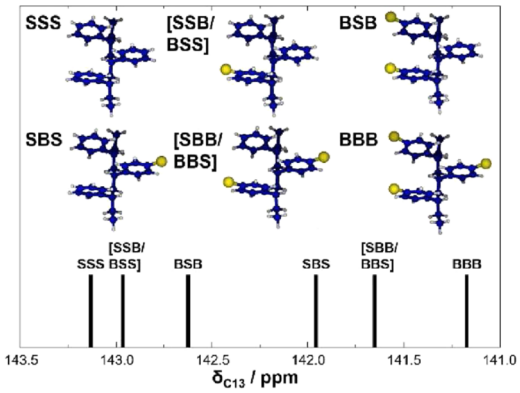

Figure 3. Theoretical chemical shifts for the quaternary carbon nuclei of the central monomer unit in the six unique triad sequences computed using electronic structure calculations. Geometries obtained at the B3LYP/def2-SVP level and NMR shielding tensors were computed using the Gauche Invariant Atomic Orbital formalism. The reported chemical shifts are referenced to a tetramethylsilane standard calculated at the same level of theory.

electronic structure calculations, the bsgHMBC experiments, and previous evidence of the low-frequency chemical shift of the quaternary carbon nucleus of a syndiotactic poly(4-bromostyrene) homopolymer[32] (where C(1′) = 143.1 ppm), groups A−F were assigned accordingly: A = S**S**S; B = [S**S**B/B**S**S]; C = B**S**B; D = S**B**S; E = [S**B**B/B**B**S]; and F = B**B**B. From these assignments, it is clear that the Blocky B-29% copolymer has a larger fraction of B**B**B triad sequences along its chains relative to the Random R-31% analogue (see Figure 1), despite their similar Br-content. Thus, the gel-state bromination results in a relatively high abundance of B**B**B triads at 29 mol % Br.

Within the groups A−F, the quaternary carbon NMR spectra in Figure 1 display multiple peaks, suggesting that the quaternary carbon nucleus is capable of communicating with its neighboring and next-neighboring styrene and Br-Sty units. Thus, the individual peaks in the NMR spectrum appear to originate from the quaternary carbon nucleus of a styrene or Br-Sty unit that exists at the center of a sequence of five monomers, i.e., a pentad, along the copolymer chain. Table 1 provides the 20 unique pentad combinations (32 total combinations) that are possible for a copolymer that contains two different monomers, grouped by triad combination and organized by the group assignments, A−F. The pentads in each group are arranged from top to bottom in the order of increasing number of Br-Sty units neighboring the central styrene or Br-Sty unit. For the [S**S**B/B**S**S]- and [S**B**B/B**B**S]-based pentads with one next-neighboring Br-Sty unit, there are two possible pentad permutations, the [s**b**ssb/b**s**sbs] ↔ [ss**s**bb/b**b**sss] and [s**b**bsb/b**s**bbs] ↔ [ss**b**bb/b**b**ss] pentads, which are ordered by increasing number of consecutive Br-Sty units. Based on the results of the theoretical chemical shifts from electronic structure calculations, which implies that bromination of a neighboring styrene unit shifts the resonance of a central styrene or Br-Sty unit to lower frequency, the order in Table 1 also represents the order anticipated for the chemical shifts of the pentad sequences, where the sssss and bb**b**bb pentads represent the highest- and lowest-frequency peaks, respectively, in the NMR spectrum.

The precise order of the pentad sequences in the NMR spectrum was further investigated by calculating the average

Table 1. Triad and Pentad Comonomer Sequences Organized by Group Assignment, A−F[a,b]

	Comonomer Sequence	
Group	Triad	Pentad
A	S**S**S	s s **s** s s s s **s** s b / b s **s** s s b s **s** s b
B	S**S**B / B**S**S	s s **s** b s / s b **s** s s s b **s** s b / b s **s** b s s s **s** b b / b b **s** s s b b **s** s b / b s **s** b b
C	B**S**B	s b **s** b s b b **s** b s / s b **s** b b b b **s** b b
D	S**B**S	s s **b** s s s s **b** s b / b s **b** s s b s **b** s b
E	B**B**S / S**B**B	s s **b** b s / s b **b** s s s b **b** s b / b s **b** b s s s **b** b b / b b **b** s s b b **b** s b / b s **b** b b
F	B**B**B	s b **b** b s s b **b** b b / b b **b** b s b b **b** b b

[a]Styrene = S or s; Br-Sty = B or b. [b]The red in the triad column is to emphasize that the peak in the NMR spectrum originates from the S or B unit that exists at the center of each triad. The red in the pentad column is to emphasize that the pentad sequences listed in each group contain the same triad sequence that is highlighted in red.

pentad sequence distribution in simulated random copolymers (r-*x*%) using a code created in-house. The code simulates 1000 copolymer chains of 1442 monomer units (based on our sPS sample, M_w = 300 K; $Đ$ = 2.0) by brominating monomers along the homopolymer chain at random up to the desired degree of bromination. Along each simulated chain, the number of each unique pentad sequence (e.g., sssss, bbbbb, etc.) is counted, starting at the first unit and moving one unit at a time along the chain. For the 12 chemically equivalent pentad sequences (e.g., sbbsb and bsbbs), the number of occurrences is added together. The prevalence of the 20 unique pentad sequences is then calculated by dividing the summed occurrences of each unique pentad sequence by the total number of pentad sequences in the chain. Thus, the relative prevalences of these 20 pentads represent the pentad sequence distribution of the simulated random chain. The average pentad sequence distribution of 1000 simulated random copolymers with 31 mol % Br-content (simulated r-31%) was calculated to compare to the experimental NMR spectrum of Random R-31%.

To compare the pentad sequence distribution of simulated r-31% to that of the real R-31% sample, the NMR spectrum of R-31% was deconvoluted into separate peak components using the line fitting function in Mestrelab Research's MestReNova x64 software. This deconvolution process was assisted by analyzing the NMR spectrum of a Random R-47% copolymer, in which the chemical shifts of 20 peaks were easily identified (see Figure S1). The chemical shifts of the peaks in the R-47% copolymer were used to define the position of the peaks in the spectrum of R-31%.

Figure 4a compares the average pentad sequence distribution of the simulated r-31% chains to the NMR spectrum of

https://dx.doi.org/10.1021/acs.macromol.0c01630
Macromolecules 2020, 53, 9539−9552

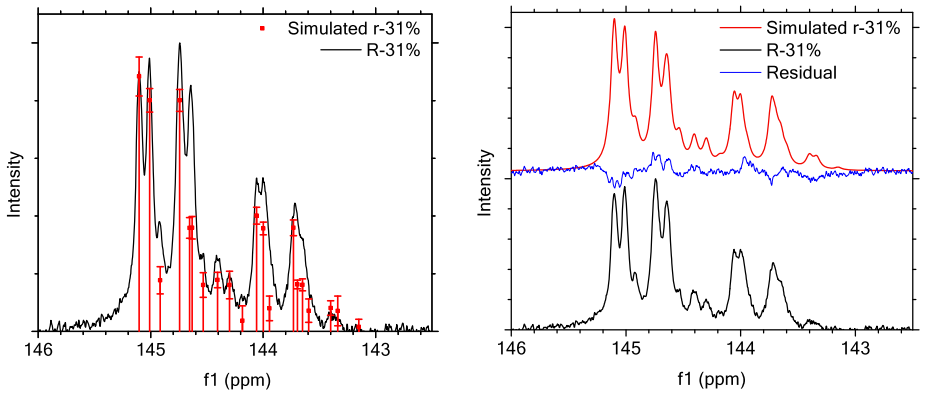

Figure 4. (a) Quaternary carbon spectrum of the Random R-31% copolymer (black line) overlaid with the average pentad sequence distribution from 1000 simulated random copolymers with 31 mol % Br-content (simulated r-31%, red vertical lines). The error bars represent ± 1 standard deviation. (b) Red lines denote the quaternary carbon spectrum of simulated r-31% calculated by applying a Lorentzian function ($LW_{1/2}$ = 8.9 Hz). The black lines denote the NMR spectrum of Random R-31%, and the blue lines denote the residual of the simulated r-31% spectrum subtracted from the R-31% spectrum.

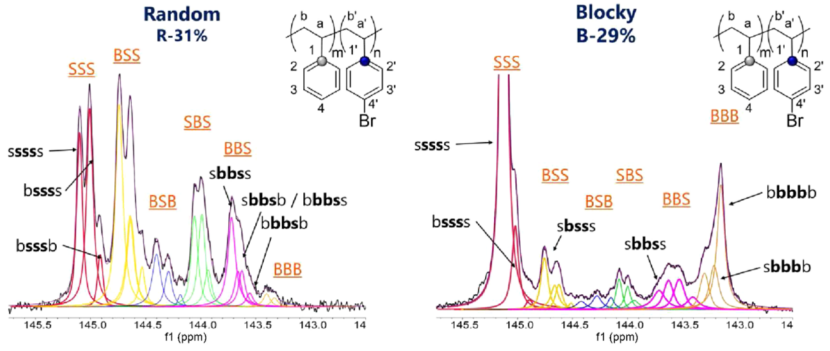

Figure 5. Quaternary carbon spectra of the Random R-31% (left) and Blocky B-29% (right) copolymers with peak fitting and assignments for the triad combinations and several of the pentad combinations.

Random R-31%. For the simulated r-31%, the relative pentad prevalences (red lines) are arranged from left to right according to the (top to bottom) order of the pentad sequences presented in Table 1 and are aligned with the peaks observed in the R-31% NMR spectrum. Based on the order of the pentad sequences presented in Table 1, the relative intensities of the pentads in the simulated r-31% appear to be in excellent agreement with the experimental Random R-31% spectrum. Figure 4b shows the average pentad sequence distribution of the simulated r-31% converted into a theoretical quaternary carbon NMR spectrum by representing each pentad prevalence line as a Lorentzian function (line width at half-max ($LW_{1/2}$) = 8.9 Hz, determined from the best fit). Again, the theoretical NMR spectrum is essentially identical to the experimental R-31% NMR spectrum, confirming that the order of the pentad sequences in Table 1 accurately represents the order of the pentad sequences in the quaternary carbon NMR spectrum.

With the confirmed assignment of the pentad resonances, it is now possible to quantify the precise sequence distributions of each of the Random and Blocky copolymers. Figure 5 shows the deconvoluted quaternary carbon NMR spectra of the Random R-31% and Blocky B-29% copolymers with color-coded triad assignments and highlighted pentad assignments. The complete pentad assignments and their chemical shifts and relative peak areas are provided in Table S1. The R-31% copolymer contains peaks with a broad distribution of intensities over the spectral range. In contrast, the B-29% spectrum contains a more bimodal distribution of peaks near the two extremes for the sssss pentad and the bbbbb pentad. This initial microstructural analysis of the NMR spectrum confirms that the bromination method manipulates the copolymer sequence; gel-state bromination produces sPS-*co*-sPS-Br copolymers with distinctly nonrandom, i.e., blocky distributions of functional groups along the chains.

The pentad sequence distribution of each of the Random and Blocky copolymers was calculated from the ratio of the area under each peak to the total area of the quaternary carbon region (142.9−145.6 ppm); see Table S2. The corresponding triad sequence distributions were tabulated from the sum of the applicable pentad prevalences, shown in Table 2. As

Table 2. Triad Sequence Distributions in the Random and Blocky Copolymers, Calculated from the Peak Integration of the Quaternary Carbon NMR Spectra

sample	SSS (%)	[SSB/BSS] (%)	BSB	SBS	[SBB/BBS] (%)	BBB (%)
B-6%	87	7	<0.5	4	1	0
B-15%	72	9	4	6	6	3
B-21%	65	8	4	5	8	10
B-29%	57	8	3	5	8	19
R-6%	85	10	<0.5	5	<0.5	0
R-16%	59	24	2	12	4	0
R-18%	54	26	3	13	4	0
R-31%	31	32	7	16	12	1

https://dx.doi.org/10.1021/acs.macromol.0c01630
Macromolecules 2020, 53, 9539−9552

expected for the Random copolymers, the prevalence of SSS triads decreases with increasing degree of bromination, while that of the BSB, SBS, [SSB/BSS], and [SBB/BBS] triads increases. The BBB triad sequence is observed only in the Random R-31% copolymer and comprises only about 1% of the total triad sequence distribution, demonstrating the low probability of brominating three consecutive monomers at random. In contrast, for the Blocky copolymers, the prevalence of SSS triads decreases to a lesser extent with increasing Br-content. In addition, above 6 mol % Br, the prevalences of the BSB, SBS, [SSB/BSS], and [SBB/BBS] triads remain relatively unchanged, while the prevalence of the BBB triad increases substantially with increasing Br-content. The larger fraction of SSS and BBB triads in the Blocky copolymers again strongly supports that these copolymers have a blocky microstructure compared to their Random copolymer analogues.

Degree of Blockiness. Using the triad sequence distributions from the experiment, the degree of blockiness in the Blocky samples was characterized by four parameters. First, the block character, R, was calculated based on Bernoullian probability statistics according to the following equation[49]

$$R = \frac{4(P_{SS})(P_{BB})}{(P_{SB})^2} \tag{2}$$

where P_{SS} = SSS + $^1/_2$ SSB; P_{BB} = BBB + $^1/_2$ SBB; and P_{SB} = 1 − P_{SS} − P_{BB}. Here, P is the probability that a polymer chain contains an SS (P_{SS}), BB (P_{BB}), or SB/BS (P_{SB}) diad, respectively. The diad probabilities are calculated from the fraction of SSS, [SSB/BSS], [SBB/BBS], and BBB triad sequences in each copolymer. For a copolymer with a Bernoullian (i.e., random) sequence distribution, the block character, R, is equal to unity. For a block-like copolymer, R is greater than unity, while for an alternating copolymer, R trends toward zero. The block character of the Random and Blocky samples and the average block character of simulated random copolymers (r-x%) are compared in Figure 6. For the simulated copolymers, R values range from 0.98 to 1.00, affirming that the simulations produce copolymers with random comonomer sequence distributions. For the Random samples, the R values vary between 0.54 (R-6%) and 0.66 (R-16%), which is similar to that expected for a random copolymer, though these data appear to suggest that in the solution-state bromination reaction, a Br-Sty unit may induce a slight inhibition in the bromination of a neighboring styrene unit. In distinct contrast to the Random copolymers, the Blocky copolymers have R values that range from ca. 3 in B-6% to ca. 25 in B-29%, which quantitatively confirms that the Blocky copolymers have distinctly block-like microstructures, even at low degrees of bromination. Interestingly, R also increases considerably with increasing Br-content, demonstrating an increase in the prevalence of consecutive styrene and consecutive Br-Sty "blocks" along the chains at high degrees of bromination. This block character, measured from the experimental NMR sequencing data, provides the first direct evidence that our postpolymerization, gel-state functionalization process[13,21,22] yields a distinctly blocky microstructure. Given the network structure of the semicrystalline gels of sPS (i.e., the heterogeneous medium for the Blocky bromination reactions), a given chain is expected to interconnect several crystallites, thus exhibiting several crystalline and amorphous segments per chain. Consequently, the large block character of Blocky B-29% suggests that the B-29% copolymer microstructure is somewhat reminiscent of a multiblock or segmented copolymer.

To obtain deeper insight into the potential lengths of the styrene and Br-Sty "blocks", in the Blocky copolymers, the average lengths of consecutive styrene units (n_S) and Br-sty units (n_B) were calculated from the triad sequence distributions according to eqs 3 and 4, respectively[48]

$$n_S = \frac{\text{SSS} + [\text{SSB/BSS}] + \text{BSB}}{\text{BSB} + \frac{1}{2}[\text{SSB/BSS}]} \tag{3}$$

$$n_B = \frac{\text{BBB} + [\text{BBS/SBB}] + \text{SBS}}{\text{SBS} + \frac{1}{2}[\text{BBS/SBB}]} \tag{4}$$

The average length of consecutive styrene and Br-sty units for the Random and Blocky copolymers is compared in Table 3. At approximately 6 mol % Br, the Random R-6% has an n_S value of ca. 18 units, which is in excellent agreement with the n_S = 17 value for a statistically random copolymer (r-6%). The Blocky B-6%, however, has a longer n_S of ca. 23 units, which

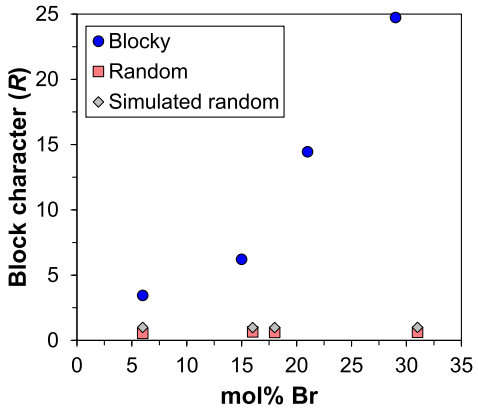

Figure 6. Block character (R) of the experimental Random (R-x%) and Blocky (B-x%) copolymers, and the simulated random (r-x%) copolymers (each an average of 1000 simulated chains) with respect to Br-content (x = Br-content).

Table 3. Average Length of Consecutive Styrene, n_S, and Br-Sty, n_B, Units and Average Number of Blocks per 100 Monomer Units, N, for the Experimental Random (R-x%) and Blocky (B-x%) Copolymers, and Theoretical Values Derived from the Average of 1000 Simulated Random Copolymers (r-x%), x = Br-Content

sample	n_S	n_B	N
B-6%	23.2	1.2	8.2
B-15%	9.7	1.7	17.5
B-21%	9.7	2.7	16.2
B-29%	10.1	3.8	14.4
R-6%	18.2	1.0	10.4
R-16%	6.0	1.1	28.0
R-18%	5.2	1.1	31.4
R-31%	3.0	1.3	46.2
r-6%	16.6	1.1	11.3
r-16%	6.2	1.2	27.0
r-18%	5.5	1.2	29.6
r-31%	3.2	1.4	42.8

https://dx.doi.org/10.1021/acs.macromol.0c01630
Macromolecules 2020, 53, 9539−9552

demonstrates that the B-6% has a higher degree of blockiness than its random analogue, even at this relatively low degree of functionalization. As the degree of bromination increases, the run lengths of consecutive styrene units (i.e., the n_S values) are expected to decrease for random functionalization. Indeed, the Random samples with greater than 6 mol % Br show a significant decrease in n_S with increasing degree of bromination. Similarly, the n_B values are expected to be near-unity and increase only slightly with the degree of bromination for the random copolymers containing up to about 30% Br-Sty comonomer (i.e., the comonomer units are essentially isolated on average). Again, the Random copolymers yield n_B values that are consistent with a random microstructure. Conversely, the Blocky samples with more than 6 mol % Br yield constant n_S values of ca. 10 units, indicating relatively long runs of consecutive styrene units in the blocky microstructure. Moreover, the n_B values are observed to increase significantly with increasing bromination. For the Blocky B-29% sample, the n_B value of 3.8 units is remarkably large and equivalent to a value expected for a random copolymer containing 73.5 mol % Br-Sty units (see Figure S2). This comparison further illustrates that the "blocks" of randomly brominated segments between the long runs of consecutive styrene units in the Blocky B-29% copolymer contain a high local density of functional groups.

The presence of relatively steady values of n_S in the Blocky samples from 15 to 29 mol % Br is suggestive of a nonhomogeneous distribution of block lengths of consecutive styrene units, where contributions from comparatively long and comparatively short blocks result in an intermediate average block length.[48] This highly segmented distribution of comonomers is consistent with the comonomer distribution anticipated for a "multiblock" copolymer prepared via postpolymerization bromination in the gel state. Again, the gel-state functionalized copolymer is likely to contain separate segments of unfunctionalized blocks that originate from the crystalline component of the gel network and randomly functionalized segments that originate from the amorphous component. For this anticipated segmented structure, it is also noted that the steady increase in n_B from ca. 1 unit in Blocky B-6% to ca. 4 units in Blocky B-29% is consistent with an increasing density of Br-Sty units in the functionalized blocks with increasing Br-content.

The N values in Table 3 represent the average number of blocks of consecutive styrene and Br-Sty units per 100 monomer units in a chain, calculated from the triad sequence distributions according to the following equation[55]

$$N = \frac{200}{n_S + n_B} \tag{5}$$

Here, a block is at least one unit. For random copolymers, it is clear that N should increase with increasing comonomer content due to an increasing number of styrene blocks that are terminated at each end by a Br-Sty unit. As expected, the Random copolymers exhibit N values that increase in a manner comparable to that of the simulated random copolymers. The Blocky samples, however, have remarkably low values of N even at high Br-content, which suggests that the Blocky copolymers contain fewer blocks per 100 monomer units (i.e., longer runs of consecutive styrene and Br-sty units along the chain). These data are consistent with a blocky copolymer microstructure that consists of long blocks of unfunctionalized styrene units and randomly functionalized segments that contain blocks of consecutive Br-Sty units that increase in length with increasing Br-content.

Simulated Chains of the Brominated sPS Copolymers. As noted above, the pentad sequence distribution provides a unique fingerprint of the copolymer microstructure and represents the average comonomer sequence distribution along a chain. Using this precise sequence information, a Fortran code was developed in-house to construct a typical copolymer chain sequence for each of the Random and Blocky copolymers (see the Supporting Information). The copolymer chain is simulated starting with a short sequence of unfunctionalized styrene units, followed by subsequent additions of short sequences of unfunctionalized and functionalized styrene units to the chain end. With each iteration of adding short sequences, the difference between the experimentally determined pentad sequence distribution and the calculated pentad sequence distribution of the simulated chain is minimized. Trials of adding sequences of 1, 3, 5, 7, 9, 11, and 13 monomers were tested to investigate the iterative addition process of the simulation code, and sequences of 7 monomers were found to minimize the residuals with respect to the experiment. Thus, the simulated chain is started with a short sequence of seven unfunctionalized styrene units and blocks of seven units are added sequentially. To add a sequence to the end of the developing chain, all possible heptad combinations (2^7 or 128) are added in turn and the deviation between the pentad sequence distribution of the intermediate chain and the experimental results is analyzed. The heptad combination that minimizes the residuals with respect to the experiment is then selectively added to the chain. The process is repeated until the chain length reaches 1442 monomers (to match our sPS sample, M_w = 300 K; $Đ$ = 2.0). It is of interest to note that the degree of functionalization in the chain is not an input parameter of this simulation. Nevertheless, the simulated chains naturally exhibit Br-Sty compositions that are in excellent agreement with experimentally measured degrees of bromination. Also, the simulated chains exhibit pentad sequence distributions that deviate by less than 1% from the experimentally determined pentad sequence distributions.

The specific output from the simulation code is a visual representation of a typical chain microstructure for each copolymer. Figure 7 displays the simulated chains that represent typical chains within the Random R-31% and Blocky B-29% copolymer samples. The root-mean-square deviations (RMSDs) between the simulated and experimental pentad sequence distributions for the simulated R-31% and B-29% chains are 0.67 and 0.57%, respectively. By inspection, it is obvious that the simulated chain representing Random R-31% contains a relatively homogeneous distribution of brominated units along the chain, as expected for a random copolymer. In addition, the simulated R-31% chain contains a large number of very short runs of consecutive styrene units (gray circles) and noticeably shorter and infrequent runs of two or more consecutive Br-Sty units (blue circles), consistent with the average block length analysis (Table 3). In distinct contrast, the simulated Blocky B-29% chain is noticeably "blocky" and exhibits numerous long blocks of styrene units and relatively long blocks of consecutive Br-Sty units. Overall, the simulated chains representing each of the Random and Blocky copolymers have decidedly different microstructures that cannot be explained by their differences in Br-content (see Figure S3); the simulated Random chains have a random

https://dx.doi.org/10.1021/acs.macromol.0c01630
Macromolecules 2020, 53, 9539−9552

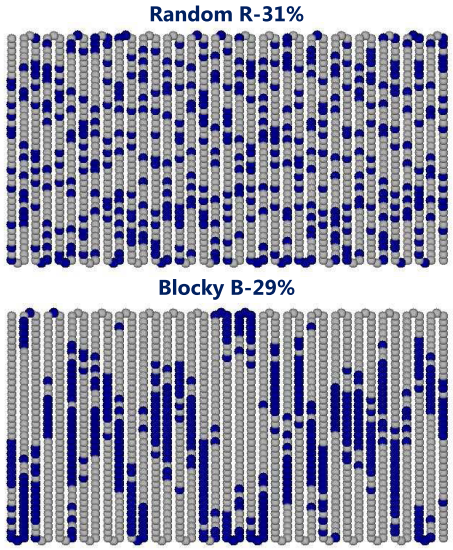

Figure 7. Simulated chains representing typical copolymer chains within the Random R-31% (top) and Blocky B-29% (bottom) samples created through an iterative process that minimizes the difference between the pentad sequence distribution of the intermediate chain and the respective data obtained directly from the experimental NMR data. Styrene units, gray circles; Br-Sty units, blue circles.

microstructure, while the simulated Blocky chains have a considerably nonrandom, i.e., blocky microstructure.

Aside from the constructive visual representations, the simulated chains provide further insight into the copolymer microstructure and the distribution of run lengths predicted to exist in copolymers prepared by the gel-state bromination method. For example, the run lengths of consecutive styrene and Br-Sty units in the simulated chains can be determined by directly counting the sequences of specific lengths, as shown in Figures S4 and S5. Table S3 displays the average lengths of consecutive styrene, n_S, and Br-Sty, n_B, units and the number of blocks per 100 units, N, found in the simulated chains representing the Random and Blocky samples. Notably, these values are in excellent agreement with the experimental n_S, n_B, and N values calculated from the NMR sequencing data, confirming the validity of the algorithm used to simulate the copolymers.

The length and distribution of consecutive styrene blocks in the simulated chains may also be used to evaluate the weight percent of styrene units that are capable of crystallizing (i.e., styrene in runs of consecutive units of sufficient length to crystallize) along the real copolymer chains. Figure 8 compares the distribution of styrene run lengths in the simulated chains representing the Random and Blocky copolymers, quantified as the weight percent of styrene units ($\%w_{Sty}$) in runs of at least block length, n. For n = 1, all styrene units in the chain are accounted for, which corresponds to a $\%w_{Sty}$ = 100 in blocks of at least one unit. As n increases, the $\%w_{Sty}$ in runs of at least n decreases. The simulated chain representing the typical Random R-6% copolymer chain exhibits 50%w_{Sty} in runs of 20−41 units. In comparison, the representative chain of Blocky B-6% exhibits half its mass of styrene in longer runs of 28−67 units, revealing its greater block character. At 16 mol % Br, the simulated Random R-16% chain contains just about one-fourth (21%w_{Sty}) of its styrene mass in runs of 12−17 units. At slightly higher Br-content, the representative chain of Random R-18% shows a sharp decrease in the longest styrene run to 12 units, which is just 7%w_{Sty}. By 31 mol % Br, the simulated chain of Random R-31% contains 50%w_{Sty} in short runs of 1−5 units. In contrast, the simulated chains representing typical chains in the 15, 21, and 29 mol % Br Blocky copolymers display half their mass of styrene in long runs of at least 28, 26, and 23 units, respectively, and all of the chains contain at least 4%w_{sty} in runs of 39 styrene units or longer. In the subsection below, this block length analysis will be correlated to copolymer crystallizability and gel morphology.

Correlation of the Simulated Chains with Respect to Experimental Results. The simulated chains provide fundamental insight into the effect of copolymer microstructure and degree of blockiness on the crystallization behavior of the copolymers after solution-state (Random) and gel-state (Blocky) functionalization. Figure 9 shows the weight percent crystallinity, $\%X_c$, of the experimental sPS homopolymer and the Random and Blocky copolymers after slow cooling (−10 °C min^{-1}) from the melt, derived from the area under the melting endotherm (ΔH_f) in the DSC heating scans with respect to the heat of fusion of 100% crystalline pure sPS[56] (ΔH_f° = 79.3 J g^{-1}), according to the relationship $\%X_c = (\Delta H_f/\Delta H_f^\circ) \times 100$. (For the DSC heating scans, see Figure S6.) At approximately 6 mol % Br, both the Random and Blocky copolymers exhibit essentially the same degree of crystallinity while slightly less than that of pure sPS. Brominated styrene units attached to sPS act as physical defects along the polymer chains, limiting crystallizability and lamellar thickness.[7,13] It is not surprising then that the Random

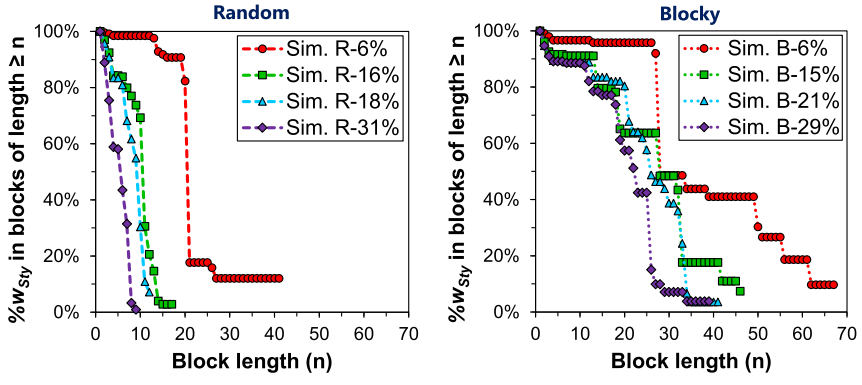

Figure 8. Weight percent of styrene units ($\%w_{Sty}$) in blocks of at least length, n, versus block length from the simulated chains representing typical chains within the Random (left) and Blocky (right) copolymer samples. The dashed lines are a guide to the eye.

https://dx.doi.org/10.1021/acs.macromol.0c01630
Macromolecules 2020, 53, 9539−9552

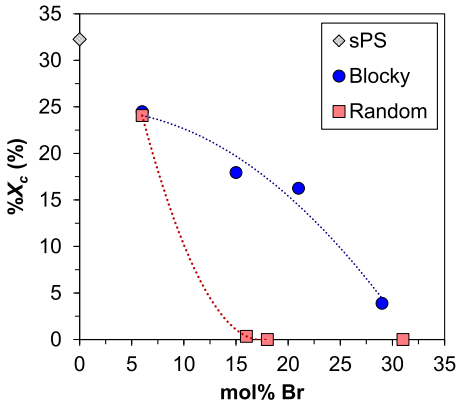

Figure 9. Weight percent crystallinity (%X_c) of the sPS homopolymer and the Random and Blocky copolymers after cooling from the melt at −10 °C min^{-1}, measured by DSC and derived from the area under the melting endotherm (ΔH_f) and the heat of fusion of 100% crystalline pure sPS[56] (ΔH_f°) according to the relationship $\%X_c = \frac{\Delta H_f}{\Delta H_f^\circ} \times 100$. The dashed lines are a guide to the eye.

and Blocky series show a depression in %X_c, with increasing Br-content as a consequence of both shorter crystallizable segments (i.e., runs of consecutive styrene units of sufficient length) and a somewhat lower occurrence of crystallizable segments along the polymer chains.

Nevertheless, at higher degrees of bromination, the Blocky copolymers are significantly more crystalline compared to the Random analogues, despite their similar Br-contents. For example, the Blocky B-21% copolymer yields a degree of crystallinity of %X_c = 16%, which constitutes 50% of the crystallinity of pure sPS, compared to %X_c < 1% for the lower Br-content Random R-16% copolymer. Beyond 16 mol % bromination, the Random copolymers were rendered amorphous and only the Blocky copolymers were capable of developing significant degrees of crystallinity under the thermal and temporal conditions of the experiment. The much greater crystallinity in the Blocky copolymers is attributed to the highly blocky microstructure that provides a significant weight percent of long styrene sequences capable of developing lamellar crystallites during the cooling process.

The enhanced crystallizability of the Blocky copolymers is in excellent agreement with the block length distributions in the simulated chains (Figure 8). Thus, the block length analysis from the simulated chains can be used to quantitatively rationalize the copolymer crystallizability. According to Flory's theory of crystallization in copolymers,[57] the probability (P_ζ) that a randomly selected styrene unit along a chain exists in a crystallizable chain segment of at least ζ styrene units is given by the following equation

$$P_\zeta = \sum_j P_{\zeta,j} = \sum_{j=\zeta}^{\infty} \frac{(j - \zeta + 1) \times w_j}{j} \quad (6)$$

where w_j is the probability that a unit chosen at random is a styrene unit in a sequence of length j, calculated by multiplying the mole fraction of styrene units (X_{Sty}) by the fraction of styrene units occurring in sequences of length j (j_{Sty}).

To estimate the average number of styrene units in a crystallizable segment in the copolymers, the lamellar thickness was probed using SAXS. The SAXS profiles of the sPS homopolymer and the Random and Blocky copolymers after 2 h isothermal crystallization from the melt at 190 °C are compared in Figure S7. The SAXS profile of the sPS homopolymer shows a weak scattering peak in the range of 0.3 nm^{-1} < q < 0.5 nm^{-1} that is attributed to intercrystalline scattering observed previously in sPS.[58] The Random R-6% and R-16% and the Blocky B-6%, B-15%, and B-21% samples also exhibit intercrystalline scattering peaks over a range of q values from 0.1 nm^{-1} < q < 0.5 nm^{-1}. The observed shift in the intercrystalline scattering feature to lower q with increasing Br-content is indicative of an increase in the center-to-center intercrystalline domain spacing, i.e., the long period (L_p). In a simple linear, two-phase model, the long period represents the sum of the thicknesses of the crystalline lamella, l_c, and the interlamellar amorphous region, l_a (such that $L_p = l_c + l_a$). The q_{max} of the scattering peak in the Lorentz-corrected SAXS profiles was used to estimate the L_p values from Bragg's law ($d_{Bragg} = 2\pi/q_{max}$). Assuming a linear two-phase model, the l_c may be estimated from the product of L_p and the volume fraction of crystallinity (X_c) within the material.[58] The average lamellar thickness was also estimated from a 1D correlation function analysis.[58] Both approaches produced similar results for the estimated average lamellar thickness and are useful for probing the average number of styrene units contained in a crystalline segment along the copolymer chain. The results of the linear two-phase approach (columns 2−7) and the 1D correlation function (columns 8 and 9) are provided in Table S4.

For the melt-crystallized sPS homopolymer and all of the Random and Blocky copolymers that demonstrate intercrystalline scattering, the estimated average thicknesses of the crystalline lamella are in the range of 4.3−5.5 nm (see Table S4). The average number of consecutive styrene units in a crystalline stem was estimated from the average lamellar thickness, based on the α-form planar zigzag structure of sPS with two monomer units per identity period (c-axis dimension = 0.51 nm).[59] Thus, based on the average lamellar thicknesses, the crystallizable samples exhibit crystalline segments of approximately 17−21 consecutive styrene units. For the purposes of this analysis, we have defined 17 consecutive sPS units as a reasonable length for a crystallizable segment (i.e., ζ = 17).

Figure 10 compares the P_ζ values calculated for the simulated chains representing the Random and Blocky copolymers. For the simulated Random copolymers, the

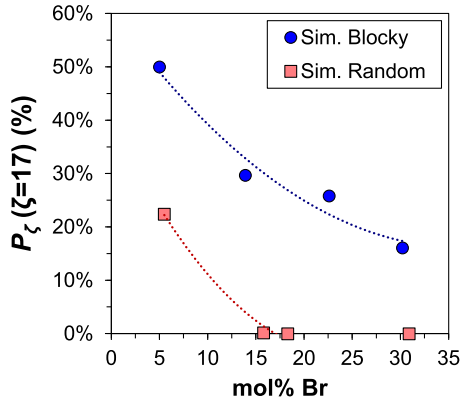

Figure 10. Probability that a randomly selected styrene unit in the simulated chains representing the Blocky (circles) and Random (squares) copolymers exists in a crystallizable chain segment, ζ, of at least 17 styrene units. The dashed lines are a guide to the eye.

https://dx.doi.org/10.1021/acs.macromol.0c01630
Macromolecules 2020, 53, 9539−9552

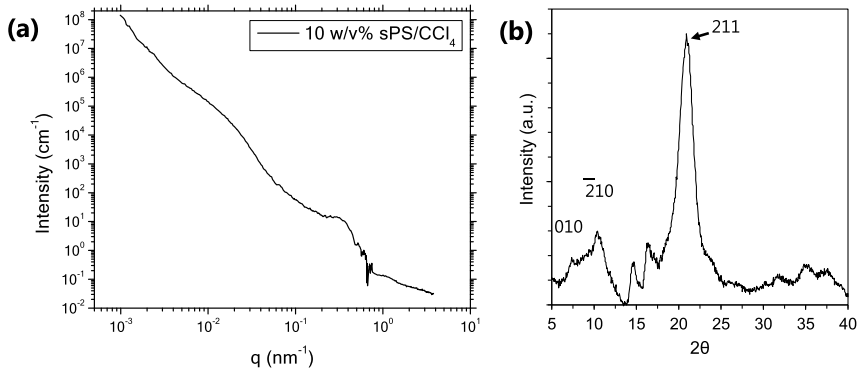

Figure 11. (a) USAXS/SAXS and (b) WAXD profiles of the 10% w/v sPS/CCl_4 gel. For the WAXD experiment, the gel was dried under vacuum at 70 °C for ca. 24 h prior to analysis.

probability of selecting a crystallizable styrene monomer (i.e., a monomer within a defect-free sequence of 17 monomer units) decreases from P_ζ = 22.40% in the simulated R-6% average chain to P_ζ = 0.14% in the simulated Random R-16% chain. This low probability of randomly encountering a styrene unit within a crystallizable styrene segment at 16 mol % Br is in excellent agreement with the experimentally determined crystallizability of the Random R-16% copolymer, which exhibits a $\%X_c$ < 1% after conditions of slow cooling from the melt. At higher degrees of bromination, this analysis predicts that the Random copolymers are no longer crystallizable.

Distinguishable from the crystallization behavior of the Random copolymers, the simulated chains representing typical chains within the Blocky samples retain greater than 15% probability that a randomly selected styrene monomer exists in a crystallizable segment, even at 29 mol % Br. This significant and relatively high probability of encountering a defect-free, crystallizable segment is in excellent agreement with the superior crystallizability of the Blocky copolymers compared to that of their Random analogues (see Figure 9). The agreement between the crystallization behavior observed in the experiment and the block length distributions of the simulated chains again validates the basis of our modeling method and strongly suggests that restricting accessibility of the functionalizing reagent to monomers in the amorphous component of the semicrystalline gel network is capable of producing copolymers with a significant reserve of crystallizable homopolymer segments.

Relationship between Gel Morphology and Copolymer Microstructure. In the gel-state functionalization process, our hypothesis has been that the gel morphology (and specifically the lamellar thickness) governs the run length of pure styrene segments in the resulting Blocky copolymers. To develop a deeper understanding of the relationship between the sPS gel morphology and the copolymer microstructure and degree of blockiness obtained after gel-state functionalization, X-ray scattering techniques were used to probe the morphology of the 10% w/v sPS/CCl_4 gels used to prepare the Blocky copolymers. The merged USAXS and SAXS profiles of the 10% w/v sPS/CCl_4 gel are shown in Figure 11a, and the WAXD profile of the gel is provided in Figure 11b. The WAXD profile exhibits crystalline reflections that are consistent with the s(2/1)2 helical conformation of the δ-form crystal structure of sPS, which is expected for this sPS/solvent gel.[18,60,61] The USAXS/SAXS profile demonstrates two scattering features: a high q scattering feature in the range of 0.2 $nm^{-1} < q < 0.7$ nm^{-1} that exhibits a q^{-4} power law dependence at higher q values and a low q scattering feature between 0.006 and 0.07 nm^{-1} that exhibits q^{-3} power law dependence in the Porod region between 0.07 and 0.15 nm^{-1}. The scattering feature at high q is consistent with the intercrystalline scattering that has been observed previously in sPS,[58] and the Porod slope of −4 is characteristic of a sharp interface expected for lamellar crystals. The q_{max} of this scattering feature, obtained from the Lorentz-corrected SAXS profile, is 0.342 nm^{-1}. The low q scattering feature is strongly suggestive of a large-scale mass fractal-type structure and is attributed to clusters or aggregates of lamellar crystallites, similar to that observed in other semicrystalline gels.[19,20] Thus, the presence of these two scattering features is strongly suggestive of an sPS/CCl_4 gel morphology consisting of clusters of crystallites that act as physical cross-links bound together by a percolating network of solvent-swollen amorphous chains. The hierarchical three-dimensional (3D) network defined by these USAXS/SAXS data constitutes the reaction media for the heterogeneous gel-state functionalization reactions.[15−19]

The average lamellar thickness in the crystalline component of the gel network was calculated using the same methods described above. The results of the SAXS analysis of the intercrystalline domain spacing are provided in Table S4. For the linear two-phase approach, two methods were used to calculate the $\%X_c$ of a desiccated sPS/CCl_4 gel: (1) DSC, obtained from the first heating trace through integration of the melting endotherm (see Figure S8); and (2) WAXD, obtained through deconvolution of the crystalline and amorphous contributions and integration. Again, the linear two-phase model approach and the 1D correlation function approach produced similar results. The estimated average lamellar thickness in the 10% w/v sPS/CCl_4 gel was found to be ca. 7.3−7.7 nm. From the average lamellar thickness, the average number of consecutive styrene units in a crystalline segment was calculated based on the helical conformation of the δ-form crystal structure of sPS with four monomer units per identity period (c-axis dimension = 0.77 nm).[59] The average crystalline segment in the crystalline lamella of the gel network contains 38−40 consecutive styrene units. This is in excellent agreement with the block lengths predicted by the simulated chains of the Blocky copolymers. Remarkably, all of the Blocky simulated chains contain one or more blocks of consecutive styrene units that are at least 39 styrene units long, even the Blocky B-29% (see Figures 8 and S4). In comparison, only the simulated chain of the low Br-content Random R-6% contains

https://dx.doi.org/10.1021/acs.macromol.0c01630
Macromolecules 2020, 53, 9539−9552

blocks of consecutive styrene units of at least 40 units. This result provides strong evidence supporting our original hypothesis that in gel-state functionalization, the average lamellar thickness in the gel governs the run length of pure sPS segments in the resulting Blocky copolymers.

CONCLUSIONS

This work demonstrates the first high-resolution comonomer sequencing of brominated sPS copolymers based on pentad assignments of the quaternary carbon region of the quantitative ^{13}C NMR spectrum. The purpose of this research was to develop a comonomer sequencing method as a means to obtain a deeper understanding of the relationship between the sPS/solvent gel morphology and the resulting copolymer microstructure and degree of blockiness in copolymers prepared by our facile heterogeneous gel-state functionalization process. Using bsgHMBC spectroscopy, electronic structure calculations, and simulated random copolymers, a comonomer sequencing method was successfully developed. As a result, every peak in the quaternary carbon region of the NMR spectrum could be assigned to a styrene or Br-Sty unit in the center of a unique combination of five monomer units, i.e., a pentad sequence. Collectively, all 20 unique pentad sequences that are possible for a copolymer that contains two different monomers were identified.

Based on the pentad sequence distributions of the Random and Blocky samples, gel-state bromination has been proven to produce copolymers with a high degree of blockiness and a high prevalence of long blocks of consecutive styrene units in a blocky microstructure. Simulated chains of each of the Random and Blocky copolymers, generated from the pentad sequence prevalences, accurately predicted that the Blocky copolymers contain a higher prevalence of crystallizable sPS segments, confirmed by the greater crystallizability of the Blocky copolymers determined from DSC experiments. Thus, the simulated chains appear to represent the microstructure of typical chains in their respective Blocky samples. Furthermore, excellent agreement between the long blocks of at least 39 consecutive styrene units in the simulated Blocky chains and the estimated number of styrene units in a crystalline segment within the sPS/CCl_4 gel of 38−40 units affirms our hypothesis that during gel-state bromination, the functionalizing reagent is impeded from reacting with monomers in the crystalline component of the gel network, producing copolymers with long blocks of unfunctionalized styrene units that originate from the crystalline segments within the crystalline lamella.

This work reveals that long segments of unfunctionalized monomer units in copolymers prepared by a gel-state, postpolymerization functionalization method originate from the precise lamellar structure within the heterogeneous gel morphology (i.e., block length is correlated with lamellar thickness). We anticipate that the ability to control the precise morphology of semicrystalline gel networks, specifically through changing the polymer concentration,[62] gelation solvent,[15,16,19,63] and/or gelation conditions,[64] will provide avenues of further investigation into tailoring the degree of blockiness in copolymers prepared by gel-state, postpolymerization functionalization processes. Future efforts will also focus on developing a robust method to simulate the gel-state, postpolymerization functionalization using the gel morphology as an input parameter, to ultimately be able to predict the copolymer microstructure and degree of blockiness of copolymers prepared from semicrystalline homopolymers that form thermoreversible gels. Given the ability to control the precise morphology of the semicrystalline gel network, the broader scope of this work is to use the fundamental information obtained from this comonomer sequencing method and simulations to guide the design and development of new functional copolymer microstructures. Specifically, this gel-state method is targeted for advanced membrane materials requiring high degrees of blocky functionality (for enhanced transport through ordered functional domains) and significant crystallinity for mechanical stability (e.g., to withstand solvent-swelling stresses during operation).

ASSOCIATED CONTENT

Supporting Information

The Supporting Information is available free of charge at https://pubs.acs.org/doi/10.1021/acs.macromol.0c01630.

Quaternary carbon NMR spectrum of R-47%, pentad chemical shifts and relative peak areas of the Random and Blocky copolymers, the theoretical average length of consecutive Br-Sty units in simulated random copolymers, simulations representing typical Random and Blocky copolymer chains and their degrees of blockiness, percent of total runs versus block length in the simulated chains, DSC heating scans, SAXS profiles and analysis of the Random and Blocky copolymers, DSC heating scan of the 10% w/v sPS/CCl_4 gel, and the Fortran code used to create the simulated chains (PDF)

AUTHOR INFORMATION

Corresponding Author

Robert B. Moore − *Department of Chemistry and Macromolecules Innovation Institute, Virginia Tech, Blacksburg, Virginia 24061, United States;* orcid.org/0000-0001-9057-7695; Email: rbmoore3@vt.edu

Authors

Kristen F. Noble − *Department of Chemistry and Macromolecules Innovation Institute, Virginia Tech, Blacksburg, Virginia 24061, United States;* orcid.org/0000-0002-1257-5085

Diego Troya − *Department of Chemistry and Macromolecules Innovation Institute, Virginia Tech, Blacksburg, Virginia 24061, United States;* orcid.org/0000-0003-4971-4998

Samantha J. Talley − *Department of Chemistry and Macromolecules Innovation Institute, Virginia Tech, Blacksburg, Virginia 24061, United States;* orcid.org/0000-0002-9415-1824

Jan Ilavsky − *X-ray Science Division, Advanced Photon Source Argonne National Laboratory, Lemont, Illinois 60439, United States;* orcid.org/0000-0003-1982-8900

Complete contact information is available at: https://pubs.acs.org/10.1021/acs.macromol.0c01630

Author Contributions

The manuscript was written by K.F.N. and R.B.M. through the contributions of all authors. D.T. developed the Fortran sequencing simulation code and DFT calculations. S.J.T. conducted the SAXS analysis. J.I. performed the USAXS/SAXS experiment. All authors have given approval to the final version of the manuscript.

https://dx.doi.org/10.1021/acs.macromol.0c01630
Macromolecules 2020, 53, 9539−9552

Funding

This material is based upon the work supported by the National Science Foundation under Grant no. DMR-1809291.

Notes

The authors declare no competing financial interest.

■ ACKNOWLEDGMENTS

This research used resources of the Advanced Photon Source, a U.S. Department of Energy (DOE) Office of Science User Facility operated for the DOE Office of Science by Argonne National Laboratory under Contract no. DE-AC02-06CH11357. The authors would like to acknowledge the use of beamline 9-ID-C for all USAXS/SAXS experiments. Advanced Research Computing at Virginia Tech is gratefully acknowledged for providing computational resources and technical support that have contributed to the results reported within this manuscript. The authors would also like to thank Virginia Tech's NMR spectroscopy facility staff, Dr. Narasimhamurthy Shanaiah and Kenneth Sharp-Knott, for their assistance with the ^{13}C and $^{1}H-^{13}C$ NMR measurements. The authors thank Dr. Gregory Fahs for developing the Mathematica code that applies the 1D correlation function algorithm to an X-ray scattering profile. The authors specially thank Dr. Alexandria Noble for developing the MatLab code that simulates random copolymers and calculates the triad and pentad sequence prevalences.

■ REFERENCES

(1) Liu, S.; Sen, A. Syntheses of Syndiotactic-Polystyrene-graft-Poly(methyl methacrylate), Syndiotactic-Polystyrene-graft-Poly(methyl acrylate), and Syndiotactic-Polystyrene-graft-Atactic-Polystyrene with Defined Structures by Atom Transfer Radical Polymerization. *Macromolecules* **2000**, *33*, 5106−5110.

(2) Semler, J. J.; Jhon, Y. K.; Tonelli, A.; Beevers, M.; Krishnamoorti, R.; Genzer, J. Facile Method of Controlling Monomer Sequence Distributions in Random Copolymers. *Adv. Mater.* **2007**, *19*, 2877−2883.

(3) Jhon, Y. K.; Semler, J. J.; Genzer, J. Effect of Solvent Quality and Chain Confinement on the Kinetics of Polystyrene Bromination. *Macromolecules* **2008**, *41*, 6719−6727.

(4) Han, J.; Jeon, B. H.; Ryu, C. Y.; Semler, J. J.; Jhon, Y. K.; Genzer, J. Discriminating Among Co-monomer Sequence Distributions in Random Copolymers Using Interaction Chromatography. *Macromol. Rapid Commun.* **2009**, *30*, 1543−1548.

(5) Jhon, Y. K.; Semler, J. J.; Genzer, J.; Beevers, M.; Gus' kova, O. A.; Khalatur, P. G.; Khokhlov, A. R. Effect of Comonomer Sequence Distribution on the Adsorption of Random Copolymers onto Impenetrable Flat Surfaces. *Macromolecules* **2009**, *42*, 2843−2853.

(6) Liu, D.; Wang, M.; Wang, Z.; Wu, C.; Pan, Y.; Cui, D. Stereoselective Copolymerization of Unprotected Polar and Nonpolar Styrenes by an Yttrium Precursor: Control of Polar-Group Distribution and Mechanism. *Angew. Chem.* **2017**, *129*, 2758−2763.

(7) Shin, J.; Chang, Y.; Nguyen, T. L. T.; Noh, S. K.; Bae, C. Hydrophilic Functionalization of Syndiotactic Polystyrene via a Combination of Electrophilic Bromination and Suzuki−Miyaura Reaction. *J. Polym. Sci., Part A: Polym. Chem.* **2010**, *48*, 4335−4343.

(8) Borriello, A.; Agoretti, P.; Ambrosio, L.; Fasano, G.; Pellegrino, M.; Venditto, V.; Guerra, G. Syndiotactic Polystyrene Films with Sulfonated Amorphous Phase and Nanoporous Crystalline Phase. *Chem. Mater.* **2009**, *21*, 3191−3196.

(9) Jeon, J. Y.; Umstead, Z.; Kangovi, G. N.; Lee, S.; Bae, C. Functionalization of Syndiotactic Polystyrene via Superacid-Catalyzed Friedel−Crafts Alkylation. *Top. Catal.* **2018**, *61*, 610−615.

(10) Jaymand, M. Recent Progress in the Chemical Modification of Syndiotactic Polystyrene. *Polym. Chem.* **2014**, *5*, 2663−2690.

(11) Loffredo, F.; Pranzo, A.; Venditto, V.; Longo, P.; Guerra, G. Clathrate Phases of Styrene/p-Methylstyrene co-Syndiotactic Copolymers. *Macromol. Chem. Phys.* **2003**, *204*, 859−867.

(12) Wei, Y.; Ke, Y.; Cao, X.; Zhang, J.; Sang, X.; Ma, Y.; Wang, F. Crystallization behaviour of syndiotactic polystyrene and benzoylated syndiotactic polystyrene. *Polymer* **2016**, *107*, 71−81.

(13) Noble, K. F.; Noble, A. M.; Talley, S. J.; Moore, R. B. Blocky bromination of syndiotactic polystyrene via post-polymerization functionalization in the heterogeneous gel state. *Polym. Chem.* **2018**, *9*, 5095−5106.

(14) Wang, Z.; Liu, D.; Cui, D. Statistically Syndioselective Coordination (Co) polymerization of 4-Methylthiostyrene. *Macromolecules* **2016**, *49*, 781−787.

(15) Mochizuki, J.; Sano, T.; Tokami, T.; Itagaki, H. Decisive Properties of Solvent Able to Form Gels with Syndiotactic Polystyrene. *Polymer* **2015**, *67*, 118−127.

(16) Shimizu, H.; Wakayama, T.; Wada, R.; Okabe, M.; Tanaka, F. Solvent Effect on Junction Size in Syndiotactic Polystyrene Physical Gel. *Polym. J.* **2005**, *37*, 294−298.

(17) Roels, T.; Deberdt, F.; Berghmans, H. Solvent Quality and Phase-Stability in Syndiotactic Polystyrene-Solvent Systems. *Macromolecules* **1994**, *27*, 6216−6220.

(18) Daniel, C.; Guerra, G.; Musto, P. Clathrate Phase in Syndiotactic Polystyrene Gels. *Macromolecules* **2002**, *35*, 2243−2251.

(19) Kobayashi, M.; Yoshioka, T.; Kozasa, T.; Tashiro, K.; Suzuki, J.; Funahashi, S.; Izumi, Y. Structure of Physical Gels Formed in Syndiotactic Polystyrene/Solvent Systems Studied by Small-Angle Neutron Scattering. *Macromolecules* **1994**, *27*, 1349−1354.

(20) Talley, S. J.; Vivod, S. L.; Nguyen, B. A.; Meador, M. A. B.; Radulescu, A.; Moore, R. B. Hierarchical Morphology of Poly(ether ether ketone) Aerogels. *ACS Appl. Mater. Interfaces* **2019**, *11*, 31508−31519.

(21) Fahs, G. B.; Benson, S. D.; Moore, R. B. Blocky Sulfonation of Syndiotactic Polystyrene: A Facile Route toward Tailored Ionomer Architecture via Postpolymerization Functionalization in the Gel State. *Macromolecules* **2017**, *50*, 2387−2396.

(22) Anderson, L. J.; Yuan, X.; Fahs, G. B.; Moore, R. B. Blocky Ionomers via Sulfonation of Poly(ether ether ketone) in the Semicrystalline Gel State. *Macromolecules* **2018**, *51*, 6226−6237.

(23) Sato, H.; Tanaka, Y.; Hatada, K. C-13 NMR analysis of polystyrene from low-molecular-weight model compounds. *J. Polym. Sci., Polym. Phys. Ed.* **1983**, *21*, 1667−1674.

(24) Chen, T. K.; Harwood, H. J. Quaternary aromatic carbon resonance spectra of epimerized isotactic polystyrene. *Makromol. Chem., Rapid Commun.* **1983**, *4*, 463−468.

(25) Ziaee, F.; Salehi Mobarakeh, H. Effect of temperature on polystyrene tacticity through para aromatic carbon splitting in 13C NMR spectroscopy. *Iran. Polym. J.* **2011**, *20*, 213−221.

(26) Suparno, S.; Lacoste, J.; Raynal, S.; Regnier, J.; Schué, F.; Sempere, R.; Sledz, J. Carbon-13 nuclear magnetic resonance spectroscopy of polystyrene. *Polym. J.* **1980**, *12*, 861−865.

(27) Cheng, H.; Lee, G. NMR studies of polystyrene tacticity. *Int. J. Polym. Anal. Charact.* **1996**, *2*, 439−455.

(28) Matsuzaki, K.; Uryu, T.; Seki, T.; Osada, K.; Kawamura, T. Stereoregularity of polystyrene and mechanism of polymerization. *Macromol. Chem.* **1975**, *176*, 3051−3064.

(29) Kawamura, T.; Toshima, N.; Matsuzaki, K. Comparison of 13C NMR spectra of polystyrenes having various tacticities and assignment of the spectra. *Macromol. Rapid Commun.* **1994**, *15*, 479−486.

(30) Feil, F.; Harder, S. New stereochemical assignments of 13C NMR signals for predominantly syndiotactic polystyrene. *Macromolecules* **2003**, *36*, 3446−3448.

(31) Nguyên-Trân, T. M.; Lauprêtre, F.; Jasse, B. Preparation and 13C NMR spectra of model compounds for poly (4-bromostyrene). *Macromol. Chem.* **1980**, *181*, 125−130.

(32) Guo, F.; Jiao, N.; Jiang, L.; Li, Y.; Hou, Z. Scandium-Catalyzed Syndiospecific Polymerization of Halide-Substituted Styrenes and Their Copolymerization with Styrene. *Macromolecules* **2017**, *50*, 8398−8405.

https://dx.doi.org/10.1021/acs.macromol.0c01630
Macromolecules 2020, 53, 9539−9552

(33) Brar, A. S.; Puneeta. Synthesis of styrene/methyl methacrylate copolymers by atom transfer radical polymerization: 2D NMR investigations. *J. Polym. Sci., Part A: Polym. Chem.* **2006**, *44*, 2076−2085.
(34) Sang, W.; Ma, H.; Wang, Q.; Hao, X.; Zheng, Y.; Wang, Y.; Li, Y. Monomer sequence determination in the living anionic copolymerization of styrene and asymmetric bi-functionalized 1, 1-diphenylethylene derivatives. *Polym. Chem.* **2016**, *7*, 219−234.
(35) Gurarslan, R.; Hardrict, S.; Roy, D.; Galvin, C.; Hill, M. R.; Gracz, H.; Sumerlin, B. S.; Genzer, J.; Tonelli, A. Beyond Microstructures: Using the Kerr Effect to Characterize the Macrostructures of Synthetic Polymers. *J. Polym. Sci., Part B: Polym. Phys.* **2015**, *53*, 155−166.
(36) Gurarslan, R.; Tonelli, A. E. An Unexpected Stereochemical Bias in the RAFT Syntheses of Styrene/p-Bromostyrene Copolymers Uncovered by the Kerr Effect. *Polymer* **2016**, *89*, 50−54.
(37) Hardrict, S. N.; Gurarslan, R.; Galvin, C. J.; Gracz, H.; Roy, D.; Sumerlin, B. S.; Genzer, J.; Tonelli, A. E. Characterizing Polymer Macrostructures by Identifying and Locating Microstructures Along Their Chains with the Kerr Effect. *J. Polym. Sci., Part B: Polym. Phys.* **2013**, *51*, 735−741.
(38) Gurarslan, R.; Gurarslan, A.; Tonelli, A. E. Characterizing Polymers with Heterogeneous Micro- and Macrostructures. *J. Polym. Sci., Part B: Polym. Phys.* **2015**, *53*, 409−414.
(39) Yang, J. C.; Jablonsky, M. J.; Mays, J. W. NMR and FT-IR Studies of Sulfonated Styrene-based Homopolymers and Copolymers. *Polymer* **2002**, *43*, 5125−5132.
(40) Dickinson, L. C.; Weiss, R.; Wnek, G. E. NMR Characterization of Sulfonation Blockiness in Copoly(styrene−sulfonated styrene). *Macromolecules* **2001**, *34*, 3108−3110.
(41) Natalello, A.; Alkan, A.; von Tiedemann, P.; Wurm, F. R.; Frey, H. Functional Group Distribution and Gradient Structure Resulting from the Living Anionic Copolymerization of Styrene and para-But-3-enyl Styrene. *ACS Macro Lett.* **2014**, *3*, 560−564.
(42) Zhang, Z.; Dou, Y.; Li, S.; Cui, D. Highly syndioselective coordination (co) polymerization of isopropenylstyrene. *Polym. Chem.* **2018**, *9*, 4476−4482.
(43) Klesper, E.; Gronski, W.; Barth, V. The kinetics and statistics of sequences during polymer analogous reaction as investigated by computer simulation. *Makromol. Chem.* **1971**, *150*, 223−249.
(44) Strickland, L. A.; Hall, C. K.; Genzer, J. Design of Copolymers with Tunable Randomness Using Discontinuous Molecular Dynamics Simulation. *Macromolecules* **2009**, *42*, 9063−9071.
(45) Shepherd, L.; Chen, T. K.; Harwood, H. J. Epimerization of isotactic polystyrene. *Polym. Bull.* **1979**, *1*, 445−450.
(46) Chen, T. K.; Gerken, T. A.; Harwood, H. J. Methylene carbon resonance spectra of epimerized isotactic polystyrene. *Polym. Bull.* **1980**, *2*, 37−42.
(47) Miller, S. A. Isotactic block length distribution in polypropylene: bernoullian vs hemiisotactic. *Macromolecules* **2004**, *37*, 3983−3995.
(48) Randall, J. C. Carbon-13 nuclear magnetic resonance quantitative measurements of average sequence lengths of like stereochemical additions in polypropylene and polystyrene. *J. Polym. Sci., Polym. Phys. Ed.* **1976**, *14*, 2083−2094.
(49) Britton, D.; Heatley, F.; Lovell, P. A. 13C NMR spectroscopy studies of branching and sequence distribution in copolymers of vinyl acetate and n-butyl acrylate prepared by semibatch emulsion copolymerization. *Macromolecules* **2001**, *34*, 817−829.
(50) Yamadera, R.; Murano, M. The determination of randomness in copolyesters by high resolution nuclear magnetic resonance. *J. Polym. Sci., Part A-1: Polym. Chem.* **1967**, *5*, 2259−2268.
(51) Frisch, M. J.; Trucks, G. W.; Schlegel, H. B.; Scuseria, G. E.; Robb, M. A.; Cheeseman, J. R.; Scalmani, G.; Barone, V.; Petersson, G. A.; Nakatsuji, H.; Li, X.; Caricato, M.; Marenich, A. V.; Bloino, J.; Janesko, B. G.; Gomperts, R.; Mennucci, B.; Hratchian, H. P.; Ortiz, J. V.; Izmaylov, A. F.; Sonnenberg, J. L.; Williams; Ding, F.; Lipparini, F.; Egidi, F.; Goings, J.; Peng, B.; Petrone, A.; Henderson, T.; Ranasinghe, D.; Zakrzewski, V. G.; Gao, J.; Rega, N.; Zheng, G.; Liang, W.; Hada, M.; Ehara, M.; Toyota, K.; Fukuda, R.; Hasegawa, J.; Ishida, M.; Nakajima, T.; Honda, Y.; Kitao, O.; Nakai, H.; Vreven, T.; Throssell, K.; Montgomery, J. A., Jr.; Peralta, J. E.; Ogliaro, F.; Bearpark, M. J.; Heyd, J. J.; Brothers, E. N.; Kudin, K. N.; Staroverov, V. N.; Keith, T. A.; Kobayashi, R.; Normand, J.; Raghavachari, K.; Rendell, A. P.; Burant, J. C.; Iyengar, S. S.; Tomasi, J.; Cossi, M.; Millam, J. M.; Klene, M.; Adamo, C.; Cammi, R.; Ochterski, J. W.; Martin, R. L.; Morokuma, K.; Farkas, O.; Foresman, J. B.; Fox, D. J. *Gaussian 16*, revision E.01; Gaussian, Inc.: Wallingford, CT, 2016.
(52) Ilavsky, J.; Zhang, F.; Andrews, R. N.; Kuzmenko, I.; Jemian, P. R.; Levine, L. E.; Allen, A. J. Development of combined microstructure and structure characterization facility for in situ and operando studies at the Advanced Photon Source. *J. Appl. Crystallogr.* **2018**, *51*, 867−882.
(53) Ilavsky, J. Nika: software for two-dimensional data reduction. *J. Appl. Crystallogr.* **2012**, *45*, 324−328.
(54) Ilavsky, J.; Jemian, P. R. Irena: tool suite for modeling and analysis of small-angle scattering. *J. Appl. Crystallogr.* **2009**, *42*, 347−353.
(55) Dasgupta, A.; Garnaik, B. Microstructures of Styrene-Acrylamide Copolymers Using ^{13}C NMR Spectroscopy. *Polym. J.* **1998**, *30*, 956.
(56) Su, C.; Jeng, U.; Chen, S.; Cheng, C.-Y.; Lee, J.-J.; Lai, Y.-H.; Su, W.; Tsai, J.; Su, A. Thermodynamic characterization of polymorphs in bulk-crystallized syndiotactic polystyrene via small/wide-angle X-ray scattering and differential scanning calorimetry. *Macromolecules* **2009**, *42*, 4200−4207.
(57) Flory, P. J. Theory of Crystallization in Copolymers. *Trans. Faraday Soc.* **1955**, *51*, 848−857.
(58) Liao, W.-P.; Lin, T.-L.; Woo, E. M.; Wang, C. Lamellar thickness of a syndiotactic polystyrene determined from small-angle X-ray scattering and transmission electron microscopy. *J. Polym. Res.* **2002**, *9*, 91−96.
(59) Albunia, A. R.; Musto, P.; Guerra, G. FTIR spectra of pure helical crystalline phases of syndiotactic polystyrene. *Polymer* **2006**, *47*, 234−242.
(60) Guerra, G.; Vitagliano, V. M.; De Rosa, C.; Petraccone, V.; Corradini, P. Polymorphisms in melt crystallized syndiotactic polystyrene samples. *Macromolecules* **1990**, *23*, 1539−1544.
(61) Daniel, C.; Giudice, S.; Guerra, G. Syndiotatic Polystyrene Aerogels with β, γ, and ϵ Crystalline Phases. *Chem. Mater.* **2009**, *21*, 1028−1034.
(62) Kobayashi, M.; Kozasa, T. Conformational ordering process on physical gelation of syndiotactic polystyrene/solvent systems revealed by time-resolved infrared spectroscopy. *Appl. Spectrosc.* **1993**, *47*, 1417−1424.
(63) Daniel, C.; Avallone, A.; Guerra, G. Syndiotactic Polystyrene Physical Gels: Guest Influence on Structural Order in Molecular Complex Domains and Gel Transparency. *Macromolecules* **2006**, *39*, 7578−7582.
(64) Daniel, C.; Menelle, A.; Brulet, A.; Guenet, J.-M. Thermoreversible gelation of syndiotactic polystyrene in toluene and chloroform. *Polymer* **1997**, *38*, 4193−4199.

https://dx.doi.org/10.1021/acs.macromol.0c01630
Macromolecules 2020, 53, 9539−9552